When fish meet a trawling vessel: examining the behaviour of gadoids using a free-floating buoy and acoustic split-beam tracking

Nils Olav Handegard and Dag Tjøstheim

Abstract: The reaction of individual gadoids to a bottom-trawling vessel has been observed in situ in the Barents Sea using a free-floating buoy and acoustic target-tracking methods. More than 20 000 tracks were analysed in terms of velocity changes in vertical, athwarthship, and alongship direction relative to the vessel, the warps, and the trawl, respectively. The fish starts diving about 15 min before vessel passing. This coincides with the time the trawl is running and not with the gradual increase in vessel noise caused by the approaching vessel. The change in horizontal movement is more gradual and is directed away from the vessel in the alongship direction, but towards the vessel in the athwarthship direction. The strongest and sharpest response is related to the trawl warps. A strong herding in front of the warps is seen. Closer to the bottom, an athwarthship herding reaction is seen away from the trawl doors or possibly the lower parts of the warps. There were only minor differences when grouping the tracks according to light level, fish size, and fish density.

Résumé : L'utilisation d'une bouée dérivante et de méthodes acoustiques de suivi de cibles dans la mer de Barents a permis d'observer in situ la réaction de gadoïdes individuels à un chalutier de fond. Nous avons ainsi analysé plus de 20 000 trajectoires en ce qui a trait aux changements de vitesse en directions verticale, perpendiculaire et parallèle au navire, aux aussières et au chalut. Le poisson commence à plonger environ 15 min avant le passage du navire. Cela coïncide avec le temps d'utilisation du chalut et non avec l'accroissement graduel du bruit causé par l'approche du navire. Le changement dans le déplacement horizontal est plus graduel et il est orienté en direction opposée au navire chez les poissons qui se déplacent parallèlement au navire et en direction du navire chez les poissons qui se déplacent perpendiculairement au navire. Les réactions les plus fortes et les plus marquées sont associées aux aussières du chalut. On observe de forts rassemblements devant les aussières. Plus près du fond, il se fait une réaction de rassemblement vers le navire pour fuir les portes du chalut ou peut-être les parties plus basses des aussières. Il n'y a que des différences mineures lorsqu'on regroupe les trajectoires en fonction du niveau de lumière, de la taille des poissons et de la densité des poissons.

[Traduit par la Rédaction]

Introduction

When demersal fish encounter a trawling vessel, it is generally acknowledged that the fish (Ona and Godø 1990) dive towards the bottom and that they may disperse horizontally. But very little is known about the details of this movement. The aim of this paper is to quantify the reaction in terms of changes in velocity components of individual fish and to relate these changes in behaviour to the different parts of the vessel and gear. More precisely, we would like to pinpoint the ranges and times at which the different segments of the reaction start and end and discuss to what extent the response is caused by stimuli such as the vessel noise, the warps, and the trawl itself. For example, is the fish reaction primarily explained by the gradual increase in vessel noise caused by the approaching vessel, or are other factors of importance? How is the reaction towards the warps and trawl doors compared with the vessel itself? Is the response directional? Is it true that the fish is primarily herded away from the vessel? This kind of quantification of fish behaviour serves a double purpose: it constitutes a framework for understanding how the fish detects and reacts to the approaching vessel, and it is important for interpreting trawl survey data on their own and in combination with acoustic information.

To achieve this goal, we collected noise data on the vessel and its gear, and the reaction of more than 20 000 fish have been monitored individually by acoustic tracking employing a split-beam echo sounder. The velocity of each fish has been decomposed in a vertical component, an alongship component, and an athwarthship component, enabling us to quantify possible avoidance–herding phenomena in three dimensions. Moreover, by using coordinate systems centred at the propeller, the warps, and the trawl doors, one can compare the strengths of directional responses due to each of these potential triggers of behavioural changes in fish.

Earlier studies of fish response towards approaching trawling vessels have mainly been based on aggregated data, such as acoustic echograms. Apparently not much progress has been made since the review by Godø (1994) a decade ago. The findings that demersal fish typically respond by swimming towards

Received 6 July 2004. Accepted 23 March 2005. Published on the NRC Research Press Web site at http://cjfas.nrc.ca/ on 24 September 2005.
J18206

N.O. Handegard.[1] Institute of Marine Research, P.O. Box 1870 Nordnes, 5817 Bergen, Norway.
D. Tjøstheim. Department of Mathematics, University of Bergen, P.O. Box 7800, 5020 Bergen, Norway.

[1]Corresponding author (e-mail: nilsolav@imr.no).

 doi: 10.1139/F05-131

the bottom (Ona and Godø 1990; Nunnallee 1991) are based on interpretations of density echograms recorded from a buoy or another vessel in the path of the approaching trawler. In addition, Ona and Godø (1990) compared the echo-integrated fish density while trawling with that in adjacent areas when cruising at normal acoustic-survey speed. They found that the echo density decreased during trawling at depths between 0 and 200 m. However, recent investigations have disputed these results to some extent (V. Hjellvik, Combining Acoustic and Trawl data for Estimating Fish Abundance (CATEFA) Project, Institute of Marine Research, P.O. Box 1870, 5817 Bergen, Norway, unpublished data).

Similar experiments have been performed for free-running vessels during acoustic surveying (i.e., without trawl). The reactions of Atlantic herring (*Clupea harengus*), Atlantic cod (*Gadus morhua*), capelin (*Mallotus villosus*), and Arctic cod (*Boreogadus saida*) were investigated by Olsen et al. (1983). More recently experiments were repeated for herring (Vabø et al. 2002). Olsen (1990) pointed out several sources of error in acoustic abundance estimates induced by fish behaviour. Soria et al. (1996) investigated the reaction of fish schools by comparing the results from a multibeam sonar with a vertical echo sounder. More recently, Fernandes et al. (2000*a*, 2000*b*) reported that fish did not avoid the noise-reduced research vessel *Scotia* by comparing the acoustic density determined by an autonomous underwater vehicle running ahead of the survey vessel with that from the vessel itself.

The methods used in these previous investigations work if the difference between true biomass and measured biomass can be established. Based on this information, inferences may be drawn about the vertical and horizontal movement of fish aggregations. However, the methods give no behavioural information in terms of velocity changes. This requires the tracking of individual fish, as done in the present paper and for which very few results are available. Engås et al. (1998) did track fish with a radio acoustic positioning system, but the sample sizes were only 13 cod. Furthermore, some preliminary results were published in Handegard et al. (2003), where a vertical diving response, consistent with Ona and Godø(1990), and a general increase in horizontal speed were found.

Materials and methods

The experiments

The R/V *G.O. Sars*, built in 1970, was used in the experiments. The vessel had 24-mm, 2.09 $kg \cdot m^{-1}$ trawl warps (wires) produced by ScanRope (Tønsberg, Norway), a Campelen 1800 shrimp trawl (Campelen, Bergen, Norway), and rockhopper gear. The trawl was equipped with a Simrad (Kongsberg Gruppen, Kongsberg, Norway) integrated trawl instrumentation (ITI) system mounted at the trawl mouth to estimate the position of the trawl relative to the vessel. A description of the ITI system is given in Engås et al. (2000). The position of the vessel was determined using the onboard global positioning system (GPS). The echo sounder provided no species information, so pelagic trawl samples using an Åkra trawl were taken in addition to the bottom trawl catches for species identification. The caught fish were mainly gadoids (Table 1), and the catches were composed of 51% (in numbers) cod, 18% haddock (*Melanogrammus aeglefinus*), and 15% saithe (pollock) (*Pollachius virens*). In addition there were 16% redfish (*Sebastes* sp.). Since cod dominated the catches and recognizing the potential bias due to varying catchability for the species involved, we assumed that the general behaviour pattern seen in our investigations can be attributed to cod.

The experiments were conducted off the coast of Finnmark (71°N, 24°–31°E) in March 2001 and April 2002. This is when immature cod prey upon capelin migrating to the shores of Finnmark for spawning, and the mature cod are spawning in the Lofoten area (Bergstad et al. 1987). The time of year, the trawl, and the species composition are representative of the Norwegian winter bottom trawl survey in the Barents Sea (Jakobsen et al. 1997). The bottom depth varied from 140 to 300 m, with a median of 290 m.

The fish reactions were measured by deploying a free-floating buoy (Bergen Acoustic Buoy; refer to Godøet al. 1999) containing a split-beam echo sounder. The rigging of the buoy and the passings were conducted as described in Handegard (2004, pp. 87–90). This buoy has a GPS, and the transducer housing contains a compass. Successive passings by the trawler were made while tracking individual fish with the buoy echo sounder. A total of 54 buoy passings were conducted. The 2001 experiments included 16 passings over seven deployments of the buoy, while in 2002, there were 38 passings over eight deployments of the buoy. In total, there were 16 daytime passings, 30 nighttime passings, and 8 twilight passings. The minimum time between passings was 50 min, the median within each deployment of the buoy being 120 min. The transducer was deployed below the buoy to avoid vessel-induced pendulum movement. The buoy–transducer depth varied between 37 and 47 m, with a median of 44 m. Wind and ocean waves can induce buoy movement, possibly affecting the transducer tilt–roll angles. To reduce this unwanted effect, we used a special buoy setup where weights and floats were used to stabilize the transducer during operation (Handegard et al. 2003, their Fig. 1).

Noise measurements of *G.O. Sars* were conducted in Stjernøyfjorden (70°13′N, 22°48′E) on 18 March 2001. A lifeboat was launched with two Brüel & Kjær (Nærum, Denmark) hydrophones (model 8106) deployed at 60 and 20 m depth. The hydrophones were connected to a Brüel & Kjær dual-channel real-time frequency analyser (model 2144) through a microphone pre-amplifier (model 5935) and type AC0101 cables, and a Sony TCD-D1 Pro-Dat tape recorder (Sony Corp., Tokyo, Japan) was used to record the data. Three passings were conducted, and the total integrated noise level in the range 40–400 Hz was calculated (Fig. 1). Events during boat handling and the start of trawling were registered, and these are indicated in the same figure. The trawl warp vibrations were measured in both passings using an accelerometer on the trawl wires. The spectrograms were obtained from the frequency analyser. Two main spectral peaks at 7 and 14 Hz were found.

Obtaining the tracks

The Simrad EK60 Scientific Echosounder (Kongsberg Gruppen) single echo detection (SED) algorithm was used to estimate the position of individual fish within the echo beam. The minimum and maximum echo length was set to 0.8 and 1.8 times

Table 1. Trawl catches in weight (W) and number (N) per nautical mile by species.

					Cod[a]		Haddock[b]		Saithe[c]		Redfish[d]	
Date	Time	Station[e]	Light level[f]	Pos[g]	W	N	W	N	W	N	W	N
March 2001												
14	0150			1	376	181	14	70	3	1	4	3
14	0757	a		0	350	195	22	107	78	59	24	30
14	1404		D	1	468	269	31	37	212	145	12	13
14	1643		N	1	535	251	40	81	10	10	5	5
14	1906	b	N	1	0	0	0	0	0	0	0	0
14	2050		N	0	119	59	8	35	11	0	6	5
14	2210		N	0	58	30	0	5	2	2	3	3
15	0030		N	1	103	53	12	58	14	11	8	8
15	0224		N	1	116	49	18	40	21	18	2	2
15	1945		N	1	150	87	27	57	17	14	4	7
15	2120		N	1	101	52	21	118	20	15	5	4
16	1903	b	N	1	0	0	0	0	0	0	0	0
16	2110	b	N	1	0	0	0	0	0	0	0	0
16	2336	a	T	0	1050	609	21	15	3	2	2	2
17	1037	b	D	1	0	0	0	0	0	0	0	0
17	1235	a	T	0	45	17	5	3	1	1	0	0
17	1807		N	1	247	126	25	25	5	4	4	4
17	2123		N	1	328	143	15	43	59	53	4	4
17	2212		N	1	229	133	22	19	23	21	18	20
April 2002												
8	1703		D	0	122	76	3	11	29	13	0	1
8	2149		N	1	1313	563	0	0	242	156	1061	1138
9	0007	b	T	1	0	0	0	0	0	0	0	0
9	0215	b	D	1	0	0	0	0	0	0	0	0
9	0426	a	T	0	643	242	30	32	4	4	0	0
9	1305		D	1	1176	889	92	174	105	88	882	1221
9	1526	b	D	1	0	0	0	0	0	0	0	0
9	1717	b	T	1	0	0	0	0	0	0	0	0
9	1844	b	T	0	0	0	0	0	0	0	0	0
9	2000	b	N	1	0	0	0	0	0	0	0	0
9	2133	b	N	0	0	0	0	0	0	0	0	0
9	2311		N	1	504	312	3	42	4	4	6	6
10	0051	b	N	1	0	0	0	0	0	0	0	0
10	0219	a	T	0	79	29	10	12	0	0	0	0
10	1357	a	T	0	142	74	55	70	4	4	0	0
10	1631	b	D	0	0	0	0	0	0	0	0	0
10	1742	b	T	1	0	0	0	0	0	0	0	0
10	1852	b	T	0	0	0	0	0	0	0	0	0
10	2023		N	1	871	553	48	123	66	52	135	148
10	2151	b	N	1	0	0	0	0	0	0	0	0
10	2338	a	T	0	37	20	15	21	0	0	0	0
12	2040		N	0	498	402	80	330	1200	612	194	246
12	2352	b	N	0	0	0	0	0	0	0	0	0
13	0034	a	T	0	16	9	2	4	1	1	0	0
13	0254	b	N	1	0	0	0	0	0	0	0	0
13	0523	b	D	1	0	0	0	0	0	0	0	0
13	0658		D	1	826	609	75	554	273	154	225	215
13	2035		N	0	122	91	1	14	13	7	1	3
13	2242		N	1	131	93	0	0	2	1	2	3
14	0035	a	T	0	7	3	6	26	0	0	0	0
14	0225		D	0	246	174	0	0	0	0	5	4

Table 1. (*concluded*)

					Cod[a]		Haddock[b]		Saithe[c]		Redfish[d]	
Date	Time	Station[e]	Light level[f]	Pos[g]	W	N	W	N	W	N	W	N
April 2002												
14	4:54		D	0	212	130	2	107	0	0	4	3
14	7:02		D	1	360	242	0	0	9	4	6	6
14	8:13		D	1	225	152	15	459	0	0	7	7
14	18:47		T	1	792	609	134	236	62	86	0	0
14	20:09	b	N	1	0	0	0	0	0	0	0	0
14	22:06		N	1	1530	671	21	29	18	7	0	0
14	23:46	a	T	0	231	126	13	16	17	19	0	0
15	2:13	b	D	1	0	0	0	0	0	0	0	0
15	3:21	b	D	1	0	0	0	0	0	0	0	0
15	18:26		T	1	1765	1605	365	599	1367	1356	10	23
15	20:15	b	N	1	0	0	0	0	0	0	0	0
15	21:46	b	N	0	0	0	0	0	0	0	0	0
15	23:11	b	N	1	0	0	0	0	0	0	0	0
16	0:23	b	T	1	0	0	0	0	0	0	0	0
16	2:55	b	D	1	0	0	0	0	0	0	0	0
Total					16 122	9928	1253	3569	3893	2925	2640	3133
Proportion (%)					67	51	5	18	16	15	11	16

[a]*Gadus morhua.*
[b]*Melanogrammus aeglefinus.*
[c]*Pollachius virens.*
[d]*Sebastes* sp.
[e]Pelagic stations for species identification are denoted "a". These are used for species identification in the upper water column and do not count as vessel–buoy passings. Bottom trawl stations with open cod end are denoted "b".
[f]Three classes of light levels: D, day; N, night; and T, twilight.
[g]Pos, position. 1 indicates that the integrated trawl instrumentation (ITI) were functioning and were consistent with detections of the warp on the echograms. 0 indicates that the ITI was not functioning or that the warp detections on the echogram were inconsistent with the ITI trawl position estimates.

the pulse length, respectively, and the maximum phase deviation and the maximum gain compensation was set to 8.0 phase steps and 6.0 dB, respectively. Next, these targets were composed into tracks using a target-tracking algorithm designed for fish observed from a moving platform (Handegard et al. 2005). This algorithm determines the correlated behaviour of targets within the echo beam and uses this to estimate the tilt–roll–heave orientation of the transducer.

The warps produce signals that could easily be misinterpreted as fish echoes. To avoid any interference with the analysis of fish behaviour, we manually removed registrations that could be interpreted as warps in every passing. The tracking is performed in a geo-referenced coordinate system, where the buoy's GPS, the transducer compass, and the tilt–roll–heave estimates are used to position each track. Fitting a regression line

$$\hat{\boldsymbol{x}}^{(i)}(t_k) = \hat{\boldsymbol{s}}_i + [t_k - \bar{t}_i]\hat{\boldsymbol{u}}_i$$

through the connected single targets has proved to be a robust method of representing each track (Handegard et al. 2005). Here, $\hat{\boldsymbol{x}}^{(i)}(t_k)$ is the estimated 3-dimensional position at time t_k of track i, $\bar{t}_i$ is the mean time point for this track, and $\hat{\boldsymbol{s}}_i$ and $\hat{\boldsymbol{u}}_i$ are parameters to be estimated. The mean time point $\bar{t}_i$ is measured relative to the vessel transducer passing of the buoy, with positive time after the buoy passing. Note that $\hat{\boldsymbol{s}}_i$ is the estimated mean position of the track, which is used to position the track in the further analysis. The parameter $\hat{\boldsymbol{u}}_i$ can be interpreted as the average velocity vector of the track. The fitting is done by least squares (i.e., by minimizing the following equation):

$$\mathrm{SS} = \sum_k \|\tilde{\boldsymbol{x}}^{(i)}(t_k) - \hat{\boldsymbol{x}}^{(i)}(t_k)\|^2$$

where $\tilde{\boldsymbol{x}}^{(i)}(t_k)$ are the measured positions from the echo sounder, and $\|\cdot\|$ is the Euclidean norm with $\|\cdot\|^2 = \sum_{j=1}^{3} x_j^2$ for $\boldsymbol{x} = [x_1\, x_2\, x_3]$ (see e.g., Handegard et al. 2003, their Fig. 2). The end result of the regression analysis for track i is that it is represented by the position–velocity pair $(\hat{\boldsymbol{s}}_i, \hat{\boldsymbol{u}}_i)$. Although the pair is estimated, to simplify, we omit the hat notation from here on.

A vessel-oriented coordinate system is used in the further analysis. The x axis is defined as the horizontal projection of the straight line from the trawl mouth to the propeller. The positive z axis is pointing from the bottom to the surface. The coordinate system is right-handed and orthogonal. Note that when changing from the geo-referenced coordinate system to the vessel-oriented coordinate system, only the direction of $\boldsymbol{u}_i$ is altered (i.e., the vessel velocity component is not included in $\boldsymbol{u}_i$). In the following analysis, the index i denoting the track number is omitted, and $\boldsymbol{s}$ and $\boldsymbol{u}$ are given relative to the vessel-oriented coordinate system.

The positioning of the vessel and gear, and thus the alignment of the vessel-oriented coordinate system, were obtained using the data from the GPS on the vessel and the Simrad Trawl Instrumentation system (ITI) on the trawl. The ITI returned

Fig. 1. Total integrated noise level between 40 and 400 Hz for the hydrophones at 20 and 40 m depth, shown as black and grey lines, respectively. Three passes were made, and this figure presents the result from the second passing. The two other passes were similar. Note that the sound levels are the absolute levels at 20 and 40 m depths, respectively, and not corrected for the distance to the vessel. Black vertical lines are events registered during the experiment.

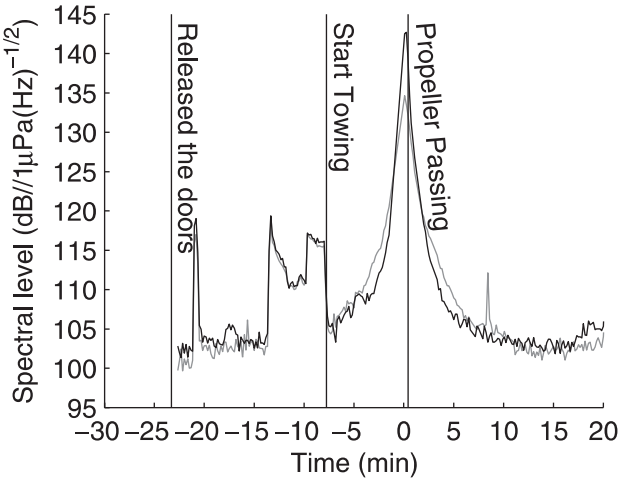

the angle and the distance to the trawl headline. In the case of failure of the ITI, the trawl was supposed to be in the path of the vessel. However, this assumption is not necessarily correct (Engås et al. 2000). The position error of each track relative to the geo-referenced coordinate system is approximately ± 40 m. The position error of the coordinate system due to an inaccurate trawl position increases with distance and is not quantified. However, a technique to verify the position estimates based on the buoy echo sounder registrations of the warps was used (Handegard 2004, pp. 87–90).

The tracks have been subjected to robustness tests involving estimated velocity, depth and current dependence, and speed of the vessel. Based on these tests, selection criteria were applied to the tracks, and those judged to be unacceptable were removed. To test the robustness of the estimated velocity, we compared the speed and horizontal direction of the original track with those of resampled subtracks. The median differences in horizontal speed and swimming angle between the resampled and original tracks were about 0.006m·s^{-1} and 10°, respectively.

The horizontal speed of a track depends on the depth, and this dependence was related to the track length. To estimate this relationship, we performed a regression of the horizontal speed $\sqrt{u_x^2 + u_y^2}$ against depth. Here u_x and u_y are x and y components of $\boldsymbol{u}$, respectively. The regression slope was recalculated after removing tracks shorter than a fixed minimum track length, thus obtaining the depth-dependent effect as a function of minimum track length. Based on this and the resampling tests, tracks shorter than 15 pings were removed. It is seen that the depth dependence is strongly reduced for the accepted tracks (Fig. 2). See the Discussion section for possible explanations of the depth effect.

When approaching the buoy, the distance and time before passing should be linearly related (i.e., the vessel should approach the buoy at constant speed). The time between the trawl

Fig. 2. The horizontal swimming speed $|v_{xy}|$ stratified in 50-m depth bins, showing increased swimming speed with depth. The boxes cover the 25th percentile, the median, and the 75th percentile, while the length of the whiskers are 1.5 times the distance between the 25th and 75th percentiles. Data points outside the whiskers are marked as +. The gray boxes show all data, while the black boxes are based on tracks with minimum track length >15 pings. The black solid line and the gray dash-dotted line show the maximum detectable linear swimming speed at a given depth assuming 1-s ping rate for the cases minimum track length >15 pings and minimum track length >2 pings, respectively.

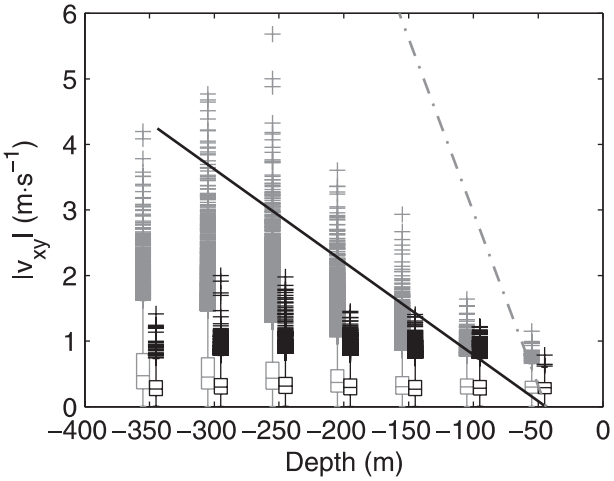

running and the vessel passing of the buoy was variable. Often the distance and time were not linearly related (Fig. 3). Looking at the position $s_x = s_{x,i}$ of track i in the alongship direction, only those tracks with s_x in the interval

$$(-v - \Delta v) \cdot t_i + x_{\text{offset}} - \Delta x < s_x < (-v + \Delta v) \cdot t_i + x_{\text{offset}} + \Delta x$$

were accepted. Here, v is the nominal vessel speed, Δv is the accepted difference in vessel speed from v, t_i is the time before–after the buoy transducer passing for track i, x_{offset} is the distance between the transducer and the propeller, and Δx is the accepted error in the position estimate in the alongship direction (Fig. 3). The parameters were set to $v = 1.54$ m·s^{-1} (3 knots), $\Delta v = 0.51$ m·s^{-1} (1 knot), $x_{\text{offset}} = 70$ m, and $\Delta x = 100$ m.

The maximum target strength (TS) was calculated along each track. This is an approximate measure of fish size. Only tracks whose maximum TS was in the interval −45 to −20 dB were accepted. This corresponds to fish lengths above ∼ 12 cm for cod (Nakken and Olsen 1977).

The measured track velocity is a combination of current drift and active swimming velocity. Unfortunately, water current measurements were not available, and a simple method to remove the current dependence was implemented. The depth-dependent mean horizontal swimming velocity from 30 to 15 min before each passing was used as an estimate of the current velocity (it is rather the mean velocity of the fish in the null situation of no vessel-related stimuli) for the passing. The depth dependence was found by binning the velocities into four depth groups. Since we are interested in fish reaction, these estimates were subtracted from the track velocities for each passing, and

Fig. 3. The alongship position s_x for each track as a function of time t before vessel–buoy passing. The black lines define the area where the tracks are valid (i.e., where the vessel is approaching the buoy at constant velocity). The gray and black dots are, respectively, the accepted and rejected tracks.

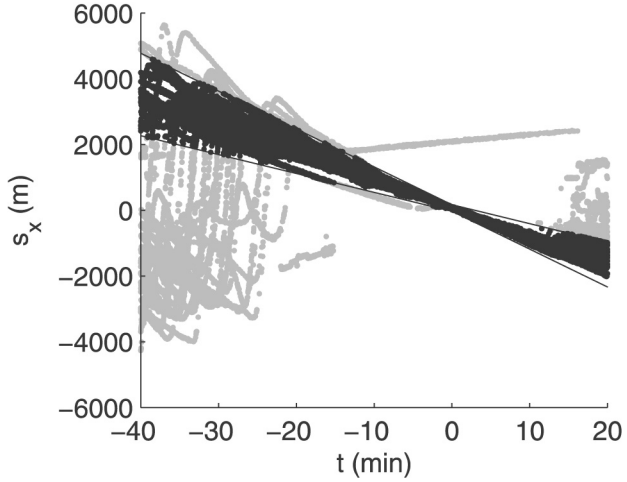

Table 2. Number of total, accepted, and rejected tracks.

All tracks	144 430
Outside path tracks	86 026
Invalid TS tracks	7 654
Short tracks	84 428
Sum of OK tracks	23 329

Note: TS, target strength.

the adjusted velocities were used in the subsequent analysis. The main analysis was based on these estimates, but as a check it was also carried through on the uncorrected data and on data adjusted by the mean null-hypothesis velocity (i.e., the velocity estimate without depth dependence).

Based on the quality screening described above, we finally kept 23 329 tracks (Table 2) with position–velocity coordinates $(\boldsymbol{s}, \boldsymbol{u})$, where the $\boldsymbol{u}$'s are corrected for water currents. In addition, we have the time $t = \bar{t}_i$, relative to vessel passing, for each track.

Response and explanatory variables

Several explanatory and response variables were derived from $\boldsymbol{s}$ and $\boldsymbol{u}$. They are based on the position $\boldsymbol{s} = [s_x\ s_y\ s_z]$ of the fish and its velocity $\boldsymbol{u} = [u_x\ u_y\ u_z]$, the estimated position of the trawl doors $\boldsymbol{x}_\mathrm{d}$, the time relative to buoy–vessel passing t, and a separate time variable, t_tow, relative to the start-towing event, with $t_\mathrm{tow} = 0$ at this event (Fig. 4).

A simple model was used to calculate the distance of each tracked fish from the trawl doors and the warps. A straight line of 60 m connects the ITI position to the doors, and one single straight line models the trawl warps (Fig. 4).

The explanatory variables are the horizontal distance to the propeller, the distance to the warps, the distance to the trawl doors, the time relative to start towing, and the time relative to buoy-vessel passing. The horizontal distance to the propeller is

Fig. 4. The vessel and gear model. The known integrated trawl instrumentation (ITI) and vessel positions are used to calculate the distance to the warp d_w, the distance to the trawl door d_tr, and the horizontal distance to the propeller d_hp. Here, $\boldsymbol{x}_\mathrm{w}$ is the point on the warp closest to the track, and $\boldsymbol{x}_\mathrm{d}$ is the estimated position of the trawl door.

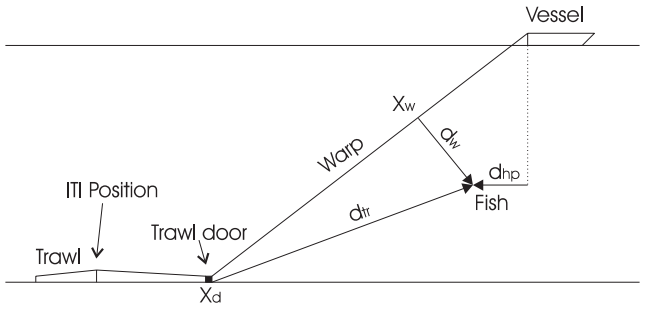

defined as

$$d_\mathrm{hp} = \mathrm{sgn}(s_x)\sqrt{s_x^2 + s_y^2}$$

where sgn is the signum function (i.e., $\mathrm{sgn}(s_x) = +1$ for $s_x \geq 0$ and $\mathrm{sgn}(s_x) = -1$ for $s_x < 0$). This means that d_hp is positive before passing and negative after. The distance to the warp is

$$d_\mathrm{w} = \|\boldsymbol{s} - \boldsymbol{x}_\mathrm{w}\| \cdot \mathrm{sgn}(s_x - x_{\mathrm{w}x})$$

where $\boldsymbol{x}_\mathrm{w}$ is the point closest to s on the line between the estimated trawl door position and the propeller position, and $x_{\mathrm{w}x}$ is the x component of $\boldsymbol{x}_\mathrm{w}$. The distance to the trawl doors is

$$d_\mathrm{tr} = \|\boldsymbol{s} - \boldsymbol{x}_\mathrm{d}\| \cdot \mathrm{sgn}(s_x - x_{\mathrm{d}x})$$

where $x_{\mathrm{d}x}$ is the x component of $\boldsymbol{x}_\mathrm{d}$. The start-towing event is the instant when the trawl is running properly, and t_tow is the time variable relative to this event. This is routinely registered for all trawl hauls conducted by Institute of Marine Research (Bergen, Norway). The time of start towing ($t_\mathrm{tow} = 0$) relative to the time the vessel passes the buoy ($t = 0$) varies between passings, and t_tow is thus not offset with a constant time relative to t. Finally, the time t before–after passing is used as an explanatory variable. Note that t is positive after the vessel passing, while the ds are negative.

The response variables are based on $\boldsymbol{u} = [u_x\ u_y\ u_z]$. To accommodate the need for an appropriate notation for the horizontal speed and the athwarthship component, it is convenient at this point to change the symbols for velocity. The vertical velocity component is denoted $v_z = u_z$, the vertical speed $|v_z| = |u_z|$, and the horizontal speed $|v_{xy}| = \sqrt{u_x^2 + u_y^2}$. Note that speed has no direction, while velocity has. To test for any horizontal directional response, we used the alongship swimming component $v_x = u_x$, and the signed athwarthship component $v_y = u_y \cdot \mathrm{sgn}(s_y)$. The signed athwarthship component is positive when a fish is swimming away from the x axis and negative when swimming towards the x axis, whereas v_x is positive when a fish is swimming in the same direction as the vessel is moving. An overview of the explanatory and response variables is given (Table 3). All these variables are contained in one data file that includes the tracks from all passings.

Table 3. The response and explanatory variables.

Response	
$\|v_z\|$	Vertical absolute speed ($m \cdot s^{-1}$)
$\|v_{xy}\|$	Horizontal absolute speed ($m \cdot s^{-1}$)
v_x	Alongship direction of u (component along x axis, positive along vessel heading)
v_y	Signed athwarthship component of u (signed component along y axis, positive perpendicular away from vessel path)
v_z	Vertical component of u (component along z axis, negative when diving)
Explanatory	
d_{hp}	Horizontal distance propeller (m) (positive in front of the vessel)
d_{w}	Distance to warp (m) (positive in front of the warp)
d_{tr}	Distance to trawl door (m) (positive in front of the vessel)
t	Time relative to vessel transducer passing (min) (negative before vessel passing)
t_{tow}	Time relative to the start trawling event (min) (negative before the start trawling event)

As potential additional explanatory variables, we have considered the light level at the sea surface, the maximum TS for each track, the mean integrated echo energy around each track, and a categorical variable indicating year 2001 or 2002. The surface light level was divided into the categories dark, light, or twilight; the diel variations were tested by analysing the dark and light groups separately. Tracks were binned into two size groups, above and below a TS threshold of $= -30$ dB, which corresponds to a cod approximately 50 cm long. The mean integrated echo energy for each track from 1 min before–after the first–last ping in the track and 10 m above–below the track was extracted. The summed energies were taken as a measure of the fish density. The data were binned into two groups, above and below the median of the integrated echo energy.

Statistical analysis

The first step of the statistical analysis was to calculate nonparametric fits between pairs of response (velocity) variables and explanatory (position–time) variables, all passings together, and then categorized on explanatory variables as defined above. Note here that modelling the response in terms of combination of variables was not instructive (see the Discussion), and the reaction is analysed in terms of each explanatory variable separately.

Two methods were used. One is a standard, nonparametric smoothing algorithm, such as the generalized additive model (GAM), to estimate the response as a function of the explanatory variables. We have used the smoothing-spline algorithm in the R program GAM module (R Development Core Team 2003). The degree of smoothing is determined using cross-validation, which results in a high degree of smoothing. The error intervals are fixed 95% confidence intervals for each value of d or t, not confidence bands.

On some occasions, the details of the response were smoothed out by the GAM. To reveal these details, we used a more or less direct extension of the method of Handegard et al. (2003), using a running mean (RM) with fixed nonoverlapping windows (Figs. 5*a*, 6*e*, and 6*f*). The estimated velocities were binned into groups referred to as running-mean windows. Outliers were eliminated by removing tracks whose variables exceeded three standard deviations. The bins themselves were nonoverlapping intervals of the explanatory variables. The steps in the time and distance variables were, respectively, $\Delta t = 1$ min and $\Delta d = 50$ m. This technique was also used for the 3D representation of the response (Fig. 7). Here the data is further divided into depth bins with steps of $\Delta z = 50$ m and distance bins with steps of $\Delta d = 100$ m.

The above-mentioned methods do not explicitly detect when the change in behaviour occurs. We are particularly interested in searching for values of the explanatory variables d or t associated with changes in the behavioural pattern. The statistical problem of finding such points of change is quite complex. In full generality, it involves piecing a series of curve segments together and assessing the presence and number of segment transitions. As a simplification, we have chosen to fit a piecewise linear function. For our data, this works well in most cases (see, e.g., Fig. 5). Several algorithms exist for fitting a series of linear regressions. We have adopted the procedure outlined in Muggeo (2003; see Appendix A). This idea goes back to Box and Tidwell (1962) and is also mentioned by McCullagh and Nelder (1989, p. 379). Muggeo (2003) has implemented an R routine "segmented", which we have adopted. The method requires a priori estimates of the breakpoints. These are determined by inspecting the nonparametric fits.

The R implementation of the segmented regression occasionally produces discontinuities in the curves (see e.g., the segmented regression line for $(t, |v_{xy}|)$ (Fig. 5b)). The curves are by definition continuous, and any gap between two consecutive fitted lines is not significant, being an artefact of the method. The gap may be assumed zero since the true lines in the underlying population are continuous.

Results

The results are presented in terms of three figures. The reaction in terms of t and the response variables gives a good overview of the larger-scale behaviour (Fig. 5), where the start is at $t = -30$ min, which corresponds to $d_{\text{hp}} \sim 900$ m. A selection of response variables as a function of distance to trawl doors and warp are presented (Fig. 6). The nonparametric spline, the fitted segmented regression lines, and the breakpoints with ± 2 SEs are displayed on these figures, and the RM curve is included in the cases where references are made in the text (Figs. 5*a*, 6*e*, and 6*f*). Finally, a three-dimensional view of the reaction is given (Fig. 7).

The fish reaction starts comparatively far away in the prevessel zone (i.e., long before the vessel transducer passes the

Fig. 5. The response variables as a function of time t (min) (*a*–*e*) and the diving v_z as a function of the t_{tow} variable (*f*). The solid lines and the dotted lines show the generalized additive model (GAM) spline curve and 95% confidence intervals, respectively. In (*a*), the gray curve is the running mean (RM) curve with standard error (± SE). In (*b*–*e*), the gray curve is the noise measurement transported from Fig. 1 based on that particular passing. The broken lines are the segmented linear regression curves. The horizontal bars in the lower parts of the panels indicate the estimated breakpoints with ±2 SEs from the segmented regression. Note that in the $|v_{xy}|$ plot (*b*), a discontinuous step is seen at the first breakpoint in the segmented regression. This is an artefact of the R-implementation method.

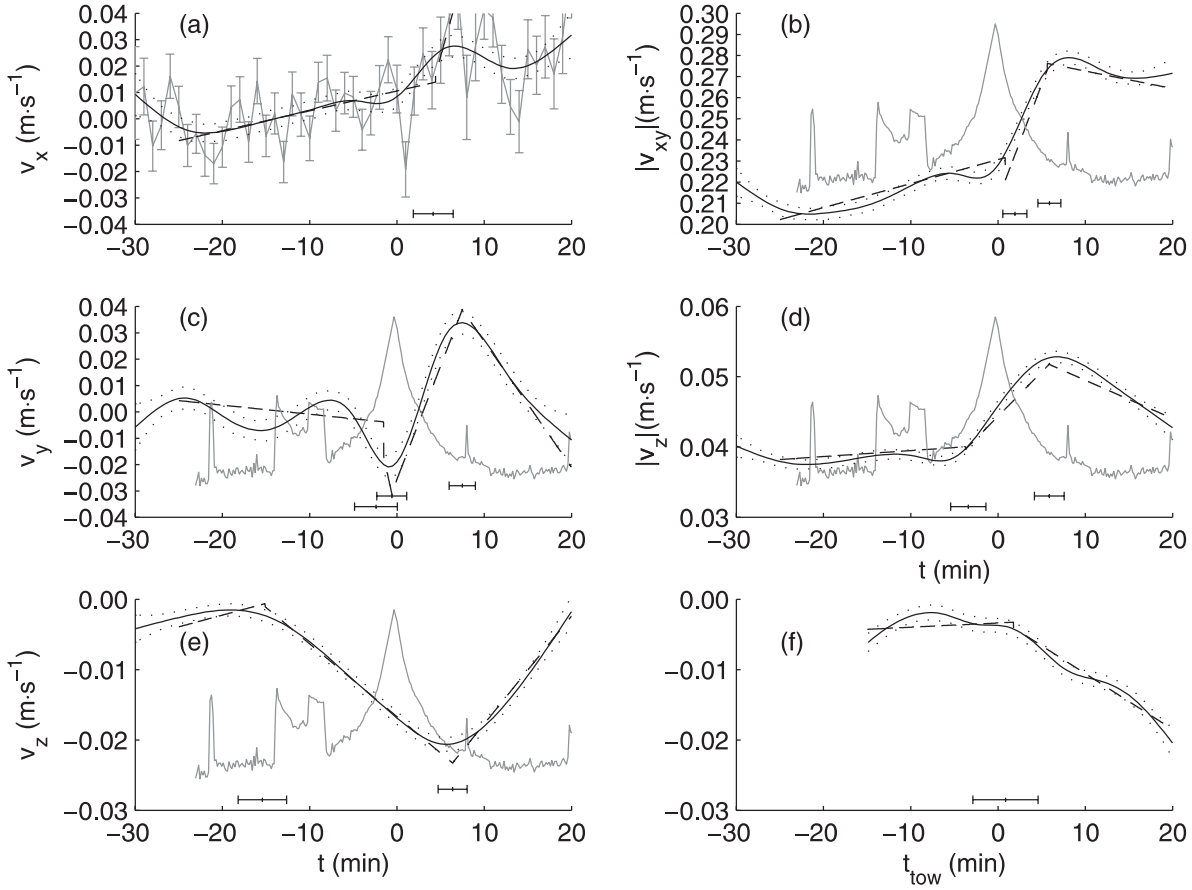

buoy (Fig. 5)). The initial response is diving, and the first breakpoint of the mean vertical component, v_z, occurs 15 min ($x_{hp} \sim$ 450 m) before the vessel passes the buoy (Fig. 5*e*). This occurs before any obvious change in vessel noise level. However, analysis of the diving response using the time variable t_{tow} reveals a clear breakpoint at $t_{tow} = 0.9 \pm 1.9$ (SE) min (i.e., at about the time the trawl starts running) (Fig. 5*f*). Note that $t_{tow} = 0$ is equivalent to the start-towing event (Fig. 1) where a steep decrease in vessel noise is seen. The absolute value of the vertical response, $|v_z|$, does not change before the vessel noise increases (Fig. 5*d*). This can be interpreted as the fish being reluctant to swim upwards in the pre-vessel zone and that the increased swimming speed does not occur before the vessel noise level increases. The time of the maximum $|v_z|$ occurs approximately 6 min after the vessel passing and does not correspond to the maximum vessel noise level.

After the initial diving response, the slope of the alongship directional response measured by v_x is significantly different from zero (Fig. 5*a*). This indicates a (weak) herding in front of the vessel, and the effect increases as the vessel approaches. The onset time for the herding effect is not detected by the segmented regression method, and the nonparametric plots suggest that there is no clear breakpoint in the pre-vessel zone. There seems to be a discontinuity (a negative step) in alongship swimming when the vessel is passing, detected by the RM curve (Fig. 5*a*). This is not seen in the GAM spline because of heavy smoothing. A negative step means that the fish changes direction from swimming with the vessel to swimming against the vessel. When using d_{hp} as an explanatory variable (not shown), this step occurred before $d_{hp} = 0$ (i.e., the fish turns towards the propeller before propeller passing). The positioning is quite accurate close to the origin of the coordinate system, and it seems that the fish reacts with a directional response towards the hull rather than towards the propeller.

The athwarthship response is negative in terms of v_y as the vessel noise increases (Fig. 5*c*) (i.e., the fish responds by swimming towards the vessel). This effect is also detected by the segmented regression. After vessel passage this changes, and there is a strong directional herding away from the vessel path.

In general, the strongest response, both vertically and horizontally, is seen after vessel passing when the vessel noise decreases. For example, the highest diving speed occurs 6 min after vessel passing. In addition, the directional polarity of this response is stronger than that of the reaction towards the vessel. There are quite similar responses to the warp and (or) trawl in terms of d_w and d_{tr} (Fig. 6). In general, the breakpoints de-

Fig. 6. The response variables v_x (*a* and *b*), v_y (*c* and *d*), v_z (*e* and *f*) as a function of the distance to the warp d_w and distance to the trawl doors d_{tr}. The solid lines and the dotted lines show the generalized additive model (GAM) spline curve and 95% confidence intervals, respectively. The horizontal bars in the lower parts of the panels indicate the estimated breakpoints with ±2 standard errors (SEs) from the segmented regression. In (*e–f*), the gray curve is the running mean (RM) curve with ±2 SEs. Note the steep response close to $d_w = 0$ m indicated by the broken lines for the segmented regression and the estimated breakpoints.

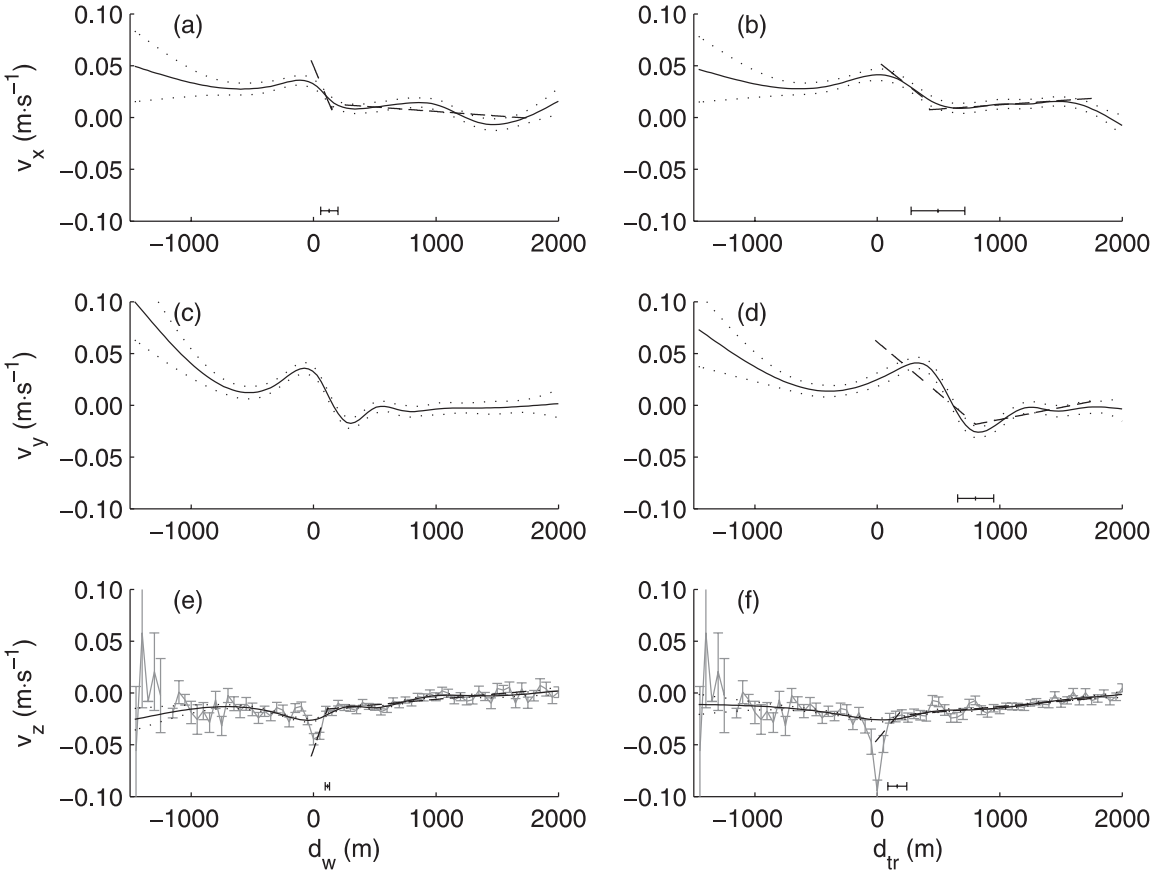

tected by the segmented regression method are located closer to $d_w = 0$ than to $d_{tr} = 0$, and the regression slopes are steeper near the warps. This is seen both for the vertical and horizontal speed (Figs. 6*b*, 6*d*). This suggests that the fish reacts rather sharply to the warps, especially seen in the diving reaction v_z (Fig. 6*e*), the vertical speed $|v_z|$ (not shown), and the alongship swimming v_x (Fig. 6*a*).

It is important to note that the directional response was not strong. The mean vertical velocity slowly decreased from 0 to ≈ -2 cm·s^{-1}, whereas the speed was an order of magnitude higher (Fig. 5), indicating a high degree of random swimming. If the (t, v_z) curve is integrated from the first reaction to the time when the trawl passes the buoy, it corresponds to a mean vertical displacement of ≈20 m. Similarly, the integrated alongship swimming over the span of the reaction indicates a mean alongship herding displacement of ≈17 m. The integrated athwarthship swimming over the duration of the fish reaction results in a mean horizontal herding displacement of only 4 m, but note that the sign is changing along the integration, thus reducing the apparent magnitude of the effect.

To further elucidate the observed reaction pattern, we provide a three-dimensional perspective of the response resolved in RM bins in depth and horizontal distance to the propeller (Fig. 7), including top, front, side, rear, and perspective view (Figs. 7*a*, 7*b*, 7*c*, 7*d*, and 7*e*, respectively). The size of the bins in depth and horizontal distance (d_{hp}) are 50 and 100 m, respectively, and the numbers of bins in depth and horizontal distance are four and ten, respectively. The cones of the figure are centred in each bin, and the depth is shown by different colour, where the upper to lower bins are shown as colours ranging from yellow to red. The response is not resolved in the athwartship direction, but is assumed to be equal on each side of the boat. The cones representing the reaction is therefore mirrored along the $x-z$ plane. The apex of the cones is pointing in the direction of the response, and the height is proportional to the magnitude of the velocity vector. This representation gives a good visualization of the observed reaction pattern close to the vessel and gear.

The response to the vessel is similar to that detected by the two-dimensional plots (Figs. 5 and 6), but with the added dimension of depth. By simultaneously assessing the alongship and athwartsip response (Figs. 7*a*, 7*b*), it may seem at first sight to correspond to the gradient of the typical butterfly sound pattern from vessels (Urick 1967, p. 273). However, at the bin of vessel passing, the response (Figs. 5*b* and 7*a*) indicates a reaction straight towards the vessel, at least in the upper layers of depth (yellow cones), thus not consistent with the butterfly pattern. The attraction component towards the vessel also occurs at the deep RM bins before and after the vessel passing

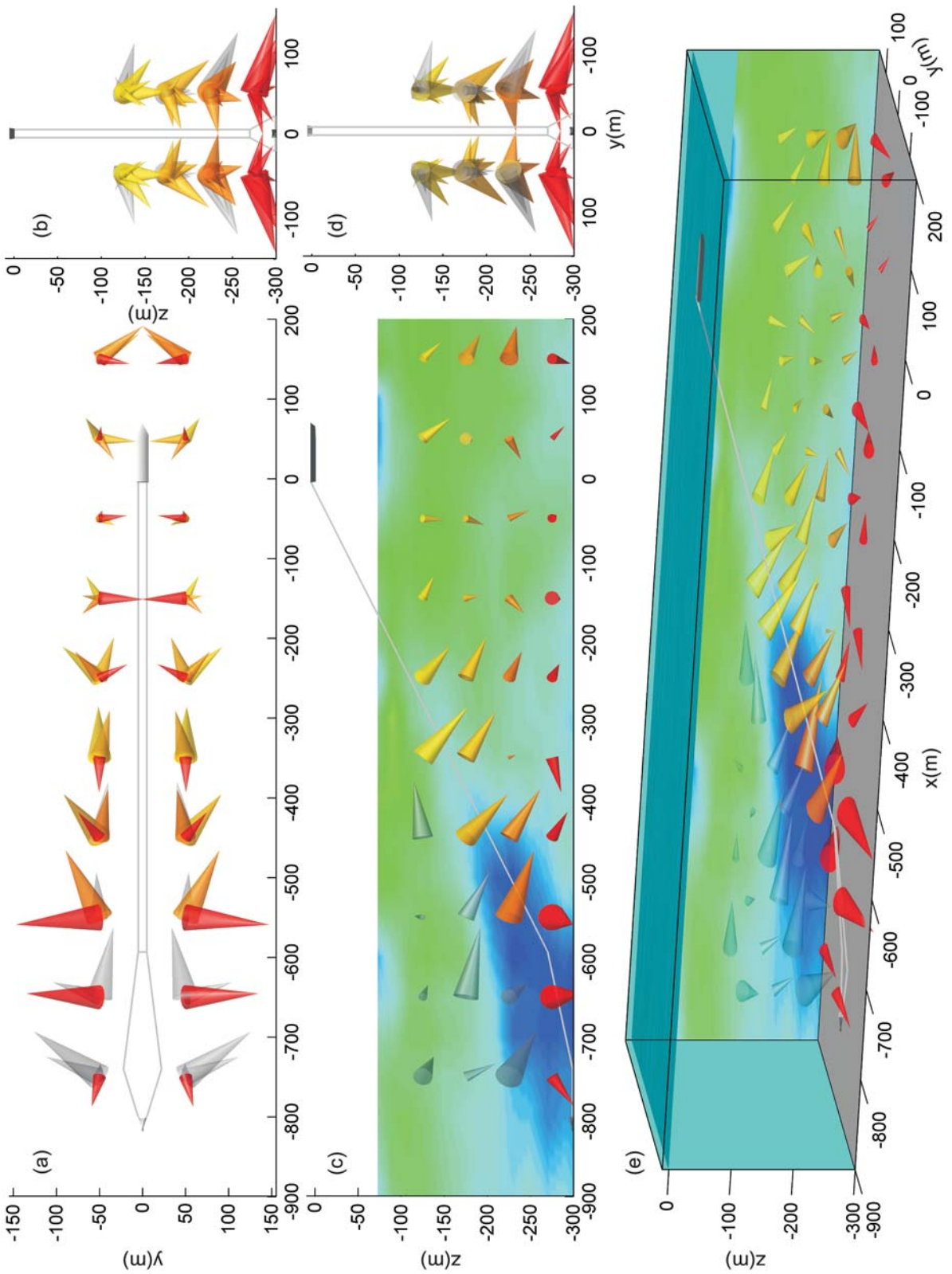

Fig. 7. The three-dimensional perspective of the directional response resolved in depth and the horizontal distance to the propeller d_{hp}: (*a*) the top view, (*b*) the front view, (*c*) the side view, (*d*) the rear view, and (*e*) shows the 3D perspective. The cones show the direction and the strength of $v = [v_x\ v_y\ v_z]$, and the colour of the cones indicate the depth bin, where red is the bottom bin and yellow is the surface bin. Gray cones indicate the bins above and after warps, where in general there are few tracks within each bin. The response is not resolved in the athwarthsip direction, and the vectors are mirrored along $y = 0$ for illustrative purposes. The swimming speed, $\sqrt{|v_{xy}|^2 + |v_z|^2}$, is shown in the background of panels (*c*) and (*e*). The range is from ~ 0.04 to ~ 0.1 m·s^{-1}.

bin (red cones at d_{hp} =150 m and d_{hp} = −50 m), where the butterfly effect is reduced.

The response towards the warps and trawl reveals a strong alongship response in the pelagic region (Fig. 7, yellow cones) and a strong athwartship reaction closer to the bottom (Fig. 7, red cones). This reaction is dominantly away from the vessel path (i.e., the opposite response to that induced by the vessel). This indicates an alongship herding response away from the warp and an athwartship herding response away from the parts of the warps closer to the bottom and possibly to the doors. After the warp has passed, fewer fish are detected. This is visualized in the plot by colouring the cones in grey scale. The swimming speed is also increased in the vicinity of the warp (Figs. 7*c*, 7*e*, background plot). Note also the general, stronger, directional response towards the warps indicated by the larger size of the cones close to the warp.

We also categorized our data according to day–night, size, density, and year-to-year effects. No clear differences were found except that both the vertical and horizontal speeds seemed generally to be higher in daytime than at night and there was a relatively small year-to-year difference for the directional response. This is especially true of the alongship response, which seems to be somewhat different in nature, not only in strength. For the athwarthship response, the strength changed but otherwise it had similar features between years.

Discussion

The method and sources of errors

The first crucial step in obtaining tracks from a split-beam echo sounder is the processing of potential targets by the SED algorithm. This algorithm fails when the fish density is high, and it is therefore difficult to make inferences about density-dependent behaviour. It may be that the critical density for more uniform behaviour is too high for the SED to work properly. This may explain why no dependence on the fish density is apparent during the vessel passings. Lowering the transducer to reduce the distance to the fish may partly solve this problem, but it would also reduce the observation volume.

If the transducer rolls cyclically, the estimated horizontal speed will increase linearly with depth. The tracker is designed to estimate and correct for this movement. In addition, for long tracks covering the period of the transducer movement, the linear regression method will average out the roll effect to a large extent, and as explained in the Materials and method section, only tracks exceeding 15 registrations have been kept. Another potential source of error is the wake-induced tilt and roll movement of the transducer as the vessel passes. This would increase the apparent horizontal speed after the vessel passing. We believe that this is not affecting our results, based on the following argument: the increase in athwarthship and alongship swimming velocity is not related to an increase in the transducer tilt–roll because the velocity increase is directional, and the faster horizontal speed seems to occur close to the warps (i.e., not in the whole water column simultaneously). Performing the analysis using different current models and adding an artificial tilt angle to the transducer do not affect the results.

So far we have discussed the implications and data correction methods applicable to a rolling transducer. However, these methods only work for periodic movements. It could be that the transducer axis is tilted off the vertical. We ran the analysis with an added constant transducer tilt of 10°. The course of the reaction was not altered, except that the mean vertical velocity changed by -0.01 m·s^{-1}. We conclude that our results and findings are not sensitive to a biased tilt angle.

The measured velocities are combinations of water currents and active fish swimming. To analyse the swimming component, a very simple depth-dependent water-current estimation technique was applied to the horizontal velocities (see the Materials and method section). In addition, we tried a current estimate with no depth dependence. This was assumed equal to the mean of the measured horizontal fish speeds in the water column. It was found that the speed estimated from the raw data was higher, but the course of the reaction was similar. This indicates that our results and conclusions are not sensitive to the water currents. However, the currents may also influence the behaviour. It has been shown that cod may utilize the tidal stream for transport (Arnold et al. 1994), and Aglen et al. (1999) showed that when the current speed increased 50 m above the bottom, the fish moved closer to the bottom. Although we are mainly interested in the vessel-induced behaviour in this paper, these effects should be taken into account when interpreting the abundance estimates from trawl surveys.

Knowledge of the positioning of the gear and vessel is discussed in Handegard (2004, pp. 87–91). In general, the accuracy is poorer, especially for the athwarthship positioning, at greater distances from the vessel. This is because the ITI measures the angle and distance to the headline of the trawl relative to the vessel. If the angular error is constant, the athwarthship positioning error increases with distance. A rather simplified model of the trawl geometry is used, but owing to the positioning error, we argue that this is adequate for our system.

The fish reaction

The noise level from the vessel is known to influence fish behaviour, and the noise level is variable between vessels and at different vessel speeds and loads (Mitson 1993; Mitson and Knudsen 2003). To overcome this problem, much effort has been made to make research vessels quieter, and the International Council for Exploration of the Sea (ICES) has made recommendations for the noise level during free running for new vessels (Mitson 1995, his fig. 22). The (former) *G.O. Sars* is a very noisy vessel (Mitson 1995, his fig. 13), but a major finding of this study was that vessel noise does not seem to explain the main features of the observed response. On the contrary, the fish seems to respond first when there is a net reduction of noise energy emitted from the vessel (in the frequency band between 40 and 300 Hz) at the start-trawling event. One explanation could be that the fish reacts to a change in noise level, even if it is a reduction. But if the fish reacts to a change, it should also react to the increase in the noise level 5–6 min before the start-towing event. Another possible explanation is that the diving response is triggered when the trawl doors hit the bottom. This may cause low frequency thuds that trigger the reaction.

It is important to note that the noise measurements were conducted in a fjord, where the noise propagation could be different from that in the open sea. This may be due to a different vertical sound speed profile, and consequently different refraction, or reflections from the boundaries of the fjord. The implication of

refraction is more prominent farther away from the source, and the measured noise level between setting the trawl and passing the buoy may not be entirely representative for the ocean experiments. However, the nature of the main increase in noise level would be similar. In addition, conductivity–temperature–depth stations at the noise measurement site and the experimental site showed similar vertical sound speed profiles.

Whether it is the sound of the trawl doors or the abrupt change in vessel noise that motivates the fish, it is evident that the handling of the boat when setting the trawl affects fish behaviour. The handling technique may be different from one skipper to another, and it is important to standardize not only the towing time and gear geometry but also the manner of controlling the trawl during the set.

Two or three minutes before vessel passing, the fish moves towards the vessel path. This is a rather counter-intuitive behavioural pattern. One explanation could be the properties of the sound field around the vessel. The propeller noise is not radiated uniformly in all directions. It is less in the fore and aft directions, probably owing to screening by the hull and the wake, respectively (Urick 1967, p. 273). This feature is used to explain the horizontal herding of pelagic species, such as herring (Misund et al. 1996) and anchovy and sardines (Soria et al. 1996), into the path of the vessel. If this is the cause, one should expect the effect to end by the time of propeller passing. The effect is reduced but not terminated at this time, and there seems to be an attraction component towards the vessel. One possible explanation is that the fish experiences the vessel as a fish-aggregating device (FAD) (S. Kaartvedt, Department of Biology, University of Oslo, P.O. Box 1064 Blindern, 0316 Oslo, Norway, personal communication) (i.e., the fish is actually attracted towards the vessel in a similar way as FADs). Previous evidence on this phenomenon is somewhat conflicting. The observed attraction towards the vessel is in contradiction to Ona and Godø (1990) and Nunnallee (1991), who reported a density draining phenomenon in front of an approaching trawler in studies of haddock and Pacific whiting (*Merluccius productus*), respectively. Ona and Godø (1990) also found a significantly lower acoustic density during trawling as compared with a free-running vessel, which they attributed to fish moving horizontally out of the vessel path. On the other hand, recent studies have shown that acoustic registrations on R/V *G.O. Sars* are in fact 10%–15% higher while trawling than when free running (V. Hjellvik, CATEFA Project, Institute of Marine Research, P.O. Box 1870, 5817 Bergen, Norway, unpublished data), whereas for the other vessels there were no significant differences between trawling and free running. This supports our findings but may indicate that it is a vessel-specific response, and not fish-specific as in the FAD hypothesis.

Reactions to the trawl warps have been reported earlier for Pacific whiting (Nunnallee 1991), but the strength and directionality of the effect were not assessed. Our analysis shows that the warps induce the strongest and sharpest reaction of the fish. The vibration of the warps generated sound with spectral peaks at 7 and 14 Hz. These frequencies are within the hearing range of cod (Sand and Karlsen 1986), and fish reaction to detectable sound at such low frequencies is believed to be strong. Enger et al. (1993) found that juvenile salmon reacted to a 10-Hz noise source, but not to one at 150 Hz. Cod are also able to sense the direction to the sound source (Schuijf and Buwalda 1975; Schuijf 1975). We did not measure the amplitude of the tones generated by the warps, but we had hoped to detect the 7- and 14-Hz peak warp vibration frequencies in the noise measurements and then correlate these with the measured reaction. We were unable to do so, possibly because other noise sources were too strong at these low frequencies. The ambient noise due to the turbulence in deep ocean currents is high at these frequencies (Urick 1967, page 164). The tones are emitted continuously, but the warp tension (and therefore the tone frequency) may vary. It has been suggested that the fish reaction may be motivated by frequency shifts in the warp vibrations (O.R. Godø, Institute of Marine Research, P.O. Box 1870, 5817 Bergen, Norway, personal communication). Unfortunately, our warp measurements were not resolved in time. Although we were not able to detect the warps from our recordings, the question still remains whether the fish is able to do so.

Another explanation of the strong response towards the warps is light, either from the surface or induced by bioluminescence. Video and flash photo observations of fish herded by the trawl doors and the trawl sweeps under different light conditions have been conducted (Wardle 1993). If the light conditions were adequate, the fish kept visual contact when avoiding the trawl door and the trailing sand cloud. This behaviour was closely related to the light level. We did analyse diel variation in the response but found little effect of time of day. Light transmitted from the surface can hardly be the explanation of our observed strong response. Another possible stimulus is bioluminescence. Indeed, the vibrating warps may generate bioluminescence, and a directional and variable response (also with year) could be expected because the bioluminescent intensity may vary with the water turbidity and the abundance of the organisms concerned. Since the vertical reaction is stable while the horizontal response varies from year to year, it could be that the horizontal directional response is predominantly triggered by bioluminescence, while the vertical response depends on the warp tones. To reach more definite conclusions about this problem, we would have to more closely investigate the warp and trawl sounds and the amount of bioluminescence in the area.

Explaining the fish reactions seen in our experiments only in terms of each stimulus separately is an oversimplification of the problem. Certainly the fish does not react to light, vessel noise, or warp tones separately, and it is probably not correct to view the response as a function of each response and explanatory variable separately. A natural approach would be to explain the response using several explanatory variables simultaneously. We tried to fit a GAM to the response variables with two or more explanatory variables, but this approach failed. The domain was not spanned properly by the explanatory variables, because of the fixed relationship between d_{hp}, d_{tr}, and to some extent d_w. Other response and explanatory variables were implemented, including the distance to the propeller and the horizontal directional swimming away from the different stimuli. These studies did not provide any new information. Consequently, the reactions were analysed in terms of a single response and explanatory variable separately.

Another simplification is the assumption that the response can be explained by the initiating stimuli alone. The internal state of fish determines the reaction thresholds of fish. If the fish changes vigilance after the approach and passing of the vessel, and as a consequence displays a stronger reaction towards the

warps, we would falsely conclude that the vessel had no impact on the reaction.

The gross features of the fish reactions are the same from year to year and from one location to another, and this is particularly true of the vertical velocity. This indicates that the measured velocity changes are largely representative of the reactions of gadoids at the time of year and in the area investigated. Thus, the findings have clear implications for the combined trawl and acoustic survey conducted in Norwegian waters during the winter (Jakobsen et al. 1997). For example, it is possible to fit the data to models for estimating parameters relevant for the trawl survey index. Some initial work has been published on this (Handegard and Tjøstheim 2004). However, the results are also of interest for the trawl capture process, and thus for trawl surveys in general. It constitutes a framework for understanding how a fish may react to an approaching vessel and suggests some implications in the way we treat the trawl as a sampling tool. For example, focus has traditionally been on selection processes close to the trawl, like herding of the sweeps (Engås and Godø 1989*a*), doors (Wardle 1993), bottom gear selection (Engås and Godø 1989*b*), and selection processes within the trawl (Marlen 2003). Little attention has been paid to the behaviour, and thus possible selection effects, before the appearance of the trawl doors. It has been mentioned by some (Dickson 1993; Graham et al. 2004) but not really addressed so far. Our results indicate that there may be a large-scale selection before the appearance of the trawl doors, and designing new sampling gear while disregarding these processes may be erroneous.

Some questions about fish behaviour were posed in the Introduction, and we are now in the position to shed some light on them. We are able to conclude that the fish reaction, in our case, were primarily not explained by the gradual increase in vessel noise as the vessel approached. The start-trawling event seemed to be the trigger that initiated the diving response. Whether this is due to trawl noise or changes in the emitted vessel noise is not clear. The induced reaction as a response to the warps and gear is stronger than that of the vessel. In addition, this response has a strong directionality. The hypothesis that a fish swims away from the vessel as a response to vessel noise seems to be false, at least in our case. The fish actually swam towards the vessel at the time of vessel passing. We have pointed to several possible explanations for this, including that it may be a vessel-specific effect. An important motivation for this study was to evaluate possible consequences for the bottom trawl survey. In this respect, the observed strong directional herding from the warps is an effect that may induce selection processes that have until now been disregarded.

Acknowledgements

We first thank Kathrine Michalsen for valuable feedback during the work. We also thank Atle Totland, Ingvald Svellingen, and the crew on R/V *G.O. Sars* for skilful handling of the buoy system, and Jan Tore Øvredal for help with the noise recordings and analysis. The Norwegian Research Council financially supported the work (Project 133426/120). This work is a part of the Dr. Scient. thesis by Nils Olav Handegard, and we thank the committee, Jens M. Hovem, Stein Kaartvedt, and Trygve Nilsen, for valuable feedback and criticism during the defence of the thesis.

References

Aglen, A., Engås, A., Huse, I., Michalsen, K., and Stensholt, B.K. 1999. How vertical distribution may effect survey results. ICES J. Mar. Sci. **56**: 345–360.

Arnold, G., Greer Walker, M., Emerson, L.S., and Holford, B.H. 1994. Movements of cod (*Gadus morhua* L.) in relation to tidal streams in the southern North Sea. ICES J. Mar. Sci. **51**: 207–232.

Bergstad, O.A., Jørgensen, T., and Dragesund, T. 1987. Life history and ecology of the gadoid resources of the Barents Sea. Fish. Res. **5**: 119–161.

Box, G., and Tidwell, P. 1962. Transformation of the independent variables. Technometrics, **4**: 431–550.

Dickson, W. 1993. Estimation of the capture efficiency of trawl gear. I: development of a theoretical model. Fish. Res. **16**: 239–253.

Enger, P.S., Karlsen, H.E., Knudsen, F.R., and Sand, O. 1993. Detection and reaction of fish to infrasound. ICES Mar. Sci. Symp.: actes du Symposium, **196**: 108–112.

Engås, A., and Godø, O.R. 1989*a*. The effect of different sweep lengths on the length composition of bottom-sampling trawl catches. J. Conseil, **45**: 263–268.

Engås, A., and Godø, O.R. 1989*b*. Escape of fish under the fishing line of a Norwegian sampling trawl and its influence on survey results. J. Conseil, **45**(3): 269–276.

Engås, A., Haugland Kyrkjebø, E., and Øvredal, J.T. 1998. Reactions of cod (*Gadus morhua* L.) in the pre-vessel zone to an approaching trawler under different light conditions. Hydrobiologia, **371–372**(1–3): 199–206.

Engås, A., Godø, O.R., and Jørgensen, T. 2000. A comparison between vessel and trawl tracks as observed by the ITI trawl instrumentation. Fish. Res. **45**: 297–301.

Fernandes, P., Brierley, A., Simmonds, E., Millard, N., McPhail, S., Armstrong, F., Stevenson, P., and Squires, M. 2000*a*. Fish do not avoid survey vessels. Nature (London), **404**: 35–36.

Fernandes, P., Brierley, A., Simmonds, E., Millard, N., McPhail, S., Armstrong, F., Stevenson, P., and Squires, M. 2000*b*. Fish do not avoid survey vessels. Nature (London), **407**: 152.

Godø, O.R. 1994. Factors affecting the reliability of groundfish abundance estimates from bottom trawl surveys. *In* Marine fish behaviour in capture and abundance estimation. *Edited by* A. Fernö and S. Olsen. Fishing News Books, Oxford, London. pp. 166–199.

Godø, O.R., Somerton, D., and Totland, A. 1999. Fish behaviour during sampling as observed from free floating buoys — application for bottom trawl survey assessment. ICES CM 1999/J:10.

Graham, N., Jones, E.G., and Reid, D.G. 2004. Review of technological advances for the study of fish behaviour in relation to demersal fishing trawls. ICES J. Mar. Sci. **61**(7): 1036–1043.

Handegard, N.O. 2004. Cod reaction to an approaching bottom trawling vessel investigated using acoustic split-beam tracking. Ph.D. thesis, Department of Mathematics, University of Bergen, Norway.

Handegard, N.O., and Tjøstheim, D. 2004. The effective swept volume of a bottom trawl. ICES CM 2004/R:07.

Handegard, N.O., Michalsen, K., and Tjøstheim, D. 2003. Avoidance behaviour in cod (*Gadus morhua*) to a bottom-trawling vessel. Aquat. Living Resour. **16**: 265–270.

Handegard, N.O., Hjellvik, V., and Patel, R. 2005. Tracking individual fish from a moving platform using a split-beam transducer. J. Acoust. Soc. Am. **118**(4). In press.

Jakobsen, T., Korsbrekke, K., Mehl, S., and Nakken, O. 1997. Norwegian combined acoustic and bottom trawl surveys for demersal fish in the Barents Sea during winter. ICES CM 1997/Y:17.

Marlen, B.v. 2003. Improving the selectivity of beam trawls in the Netherlands: the effect of large mesh top panels on the catch rates of sole, plaice, cod and whiting. Fish. Res. **63**(2): 155–168.

McCullagh, P., and Nelder, J. 1989. Generalized linear models. Chapman & Hall, London.

Misund, O.A., Øvredal, J.T., and Hafsteinsson, M.T. 1996. Reactions of herring schools to the sound field of a survey vessel. Aquat. Living Resour. **9**: 5–11.

Mitson, R.B. 1993. Underwater noise radiated by research vessels. ICES Mar. Sci. Symp.: actes du Symposium, **196**: 147–152.

Mitson, R.B. **1995**. Underwater noise of research vessels, review and recommendations. Int. Counc. Explor. Sea (ICES) Coop. Res. Rep. No. 209.

Mitson, R.B., and Knudsen, H.P. 2003. Causes and effects of underwater noise on fish abundance estimation. Aquat. Living Resour. **16**: 255–263.

Muggeo, V.M.R. 2003. Estimating regression models with unknown break points. Stat. Med. **22**: 3055–3071.

Nakken, O., and Olsen, K. 1977. Target strength measurements of fish. Rapp. P.-V. Reun. Cons. Int. Explor. Mer, **189**: 147–158.

Nunnallee, E.P. 1991. An investigation of the avoidance reactions of Pacific whiting (*Merluccius productus*) to demersal and midwater trawl gear. ICES CM 1991/B:5.

Olsen, K. 1990. Fish behaviour and acoustic sampling. Rapp. P.-V. Reun. Cons. Int. Explor. Mer, **189**: 147–158.

Olsen, K., Angell, J., Pettersen, F., and Løvik, A. 1983. Observed fish reactions to a surveying vessel with special reference to herring, cod, capelin and polar cod. FAO Fish. Rep. **300**.

Ona, E., and Godø, O.R. 1990. Fish reaction to trawling noise: the significance for trawl sampling. Rapp. P.-V. Reun. Cons. Int. Explor. Mer, **189**: 159–166.

R Development Core Team. 2003. R: a language and environment for statistical computing. R Foundation for Statistical Computing, Vienna, Austria. ISBN 3-900051-00-3.

Sand, O., and Karlsen, H.E. 1986. Detection of infrasound by the Atlantic cod. J. Exp. Biol. **125**: 197–204.

Schuijf, A. 1975. Directional hearing of cod (*Gadus morhua* L.) under approximate free field conditions. J. Comp. Physiol. **98**: 333–343.

Schuijf, A., and Buwalda, R. 1975. On the mechanics of directional hearing in cod (*Gadus morhua* L.). J. Comp. Physiol. **98**: 307–332.

Soria, M., Fréon, P., and Gerlotto, F. 1996. Analysis of vessel influence on spatial behaviour of fish schools using a multi-beam sonar and consequences for biomass estimates by echo-sounder. ICES J. Mar. Sci. **53**: 453–458.

Urick, R.J. 1967. Principles of underwater sound for engineers. McGraw-Hill, New York.

Vabø, R., Olsen, K., and Huse, I. 2002. The effect of vessel avoidance of wintering Norwegian spring spawning herring. Fish. Res. **58**: 59–77.

Wardle, C.S. 1993. Fish behaviour and fishing gear. *In* Behaviour of teleost fishes. *Edited by* T.J. Pitcher. Chapman & Hall, London. Fish Fish. Ser. **7**: 609–644.

Appendix A. Fitting the segmented regression model.

The segmented regression line model for v_z with breakpoints ψ_1, ψ_2, etc., is given by

$$v_z = \alpha t + \sum_i \beta_i (t - \psi_i) I(t > \psi_i)$$

where I is an indicator variable, α is the slope of the line segment prior to ψ_1, and β_1 is the difference in slope parameter for $t > \psi_1$ and $t < \psi_2$. If more than one breakpoint is searched, β_2 is the next change in slope, continuing until all the breakpoints are determined. When using the positions as explanatory variables, t is replaced by d, and for the other responses, v_z is replaced with the desired response variable. Note that our interest is primarily in the change points ψ_i rather than the regression parameters α and β_i. The regression model is nonlinear with respect to ψ_i. Linearization of the model around the estimated breakpoint $\hat{\psi}_i^{(k-1)}$, obtained at stage $k-1$ of the iterative procedure, yields

$$v_z = \alpha t + \sum_i \beta_i [t - \hat{\psi}_i^{(k-1)}] I[t > \hat{\psi}_i^{(k-1)}] + \sum_i \gamma_i I[t > \hat{\psi}_i^{(k-1)}]$$

where $\gamma_i = \beta_i[\psi_i - \psi_i^{(k-1)}]$. The problem is now reduced to a multiple linear regression. It is seen that for v_z the breakpoints can be expected around $t = -15$ and $t = 5$ min (Fig. 5*e*), and these are chosen as initial estimates $\psi_1^{(0)} = -15$ and $\psi_2^{(0)} = 5$, respectively. Every iteration yields least-squares estimates of $\hat{\alpha}_i^{(k-1)}$, $\hat{\beta}_i^{(k-1)}$, $\hat{\gamma}_i^{(k-1)}$, and subsequently $\hat{\psi}_i^{(k)} = [\hat{\gamma}_k^{(k-1)}/\hat{\beta}_k^{(k-1)}] + \hat{\psi}_i^{(k-1)}$. The iteration procedure terminates when $\hat{\psi}_i^{(k)} - \hat{\psi}_i^{(k-1)} = [\hat{\gamma}_i^{(k-1)}/\hat{\beta}_i^{(k-1)}]$ is deemed sufficiently small, at which stage we take $\hat{\alpha}_i = \hat{\alpha}_i^{(k-1)}$, $\hat{\beta}_i = \hat{\beta}_i^{(k-1)}$, and $\hat{\psi}_i = \hat{\psi}_i^{(k)}$. Note that this method assumes that change points exist, such that $\beta_i > 0$. We are not concerned with testing for the existence of change points.

Standard errors for the estimates can be found by bootstrapping, but following (Muggeo 2003) we chose to be guided by asymptotic analysis. The errors of $\hat{\alpha}_i$ and $\hat{\beta}_i$ are obtained by maximum likelihood and that of $\hat{\psi}_i$ by the delta method based on $\hat{\psi}_i = (\hat{\gamma}_i/\hat{\beta}_i) + \psi_i$. It should be noted that these formulae require a large number of tracks in each linear segment to obtain the derived asymptotic distribution as a reasonable approximation. This means that the p values of the estimated regression parameters should be interpreted with caution. Typically, the number of tracks for each regression segment is between 1000 and 15 000, which would be sufficient, but we also have segments with fewer observations.